

Characterization of an acyl-coenzyme A binding protein predominantly expressed in human primitive progenitor cells[§]

Eric Soupene,¹ Vladimir Serikov, and Frans A. Kuypers

Children's Hospital Oakland Research Institute, Oakland, CA 94609

Abstract Human acyl-coenzyme A binding domain-containing member 6 (ACBD6) is a modular protein that carries an acyl-CoA binding domain at its N terminus and two ankyrin motifs at its C terminus. ACBD6 binds long-chain acyl-CoAs with a strong preference for unsaturated, C18:1-CoA and C20:4-CoA, over saturated, C16:0-CoA, acyl species. Deletion of the C terminus, which is not conserved among the members of this family, did not affect the binding capacity or the substrate specificity of the protein. ACBD6 is not a ubiquitous protein, and its expression is restricted to tissues and progenitor cells with functions in blood and vessel development. ACBD6 was detected in bone marrow, spleen, placenta, cord blood, circulating CD34⁺ progenitors, and embryonic-like stem cells derived from placenta. In placenta, the protein was only detected in CD34⁺ progenitor cells present in blood and in CD31⁺ endothelial cells surrounding the blood vessels. These cells were also positive for the marker CD133, and they probably constitute hemangiogenic stem cells, precursors of both blood and vessels. **¶** We propose that human ACBD6 represents a cellular marker for primitive progenitor cells with functions in hematopoiesis and vascular endothelium development.—Soupene, E., V. Serikov, and F. A. Kuypers. Characterization of an acyl-coenzyme A binding protein predominantly expressed in human primitive progenitor cells. *J. Lipid Res.* 2008. 49: 1103–1112.

Supplementary key words placenta • endothelial cells • vascular development • stem cells

Acyl-coenzyme A binding proteins (ACBPs) play a role in the sequestration, transport, and distribution of long-chain acyl-CoAs in cells (1–4). Long-chain acyl-CoA esters can be inhibitory for the activity of acyl-CoA-producing enzymes (3, 5), and binding to ACBPs opposes product feedback inhibition. Conversely, acyl-CoAs bound to acyl-CoA binding proteins appear to represent the preferred

form of the substrate for acyl-CoA-utilizing enzymes (5, 6). It has also been suggested that the acyl-CoA/ACBP complex interacts with utilizing enzymes (7). In addition, the detergent nature of free acyl-CoAs can be quenched by binding to these proteins, in the same manner as BSA neutralizes circulating free acyls and acyl-CoAs.

Long-chain acyl-CoAs are intermediates in lipid metabolism and can also be signaling molecules involved in metabolism and gene regulation (4, 8). Regulatory functions of the ACBP proteins are indicated by their interaction with other proteins, such as the γ -aminobutyric acid receptor GABA_A (3, 9–11), Numb proteins in neural progenitors (12), the Golgi membrane protein GOLGA3 (13), and the ethylene-responsive element binding protein in Arabidopsis (AtEBP) (14). In addition, the different members of the plant ACBP family have been localized in the cytosol (15), associated with the plasma membrane, intracellular vesicles, and organelles (16, 17), and secreted extracellularly (18). In mammals, change in the subcellular distribution of member 3, ACBD3, from the Golgi apparatus to the cytosol during the cell cycle regulates the self-renewal of neural stem cells (12).

In mammals, there are six members of the acyl-CoA binding domain-containing (ACBD) family, and their annotation is not uniform. All six ACBD proteins contain an ACB domain at the N terminus, but they do not share significant homology at the C-terminal region. Member 1, diazepam binding inhibitor (or ACBP), is the shortest of the family and lacks the extended C terminus present in the other members (1, 3, 19). Member 2, peroxisomal enoyl-CoA isomerase, contains an enoyl-CoA hydratase/carnitine racemase domain and represents a multifunctional enzyme with acyl-CoA binding capacity and a Δ^3, Δ^2 -enoyl-CoA isomerase activity (20–22). Member 3, ACBD3 (or Golgi complex-associated protein of 60 kDa, GCP60), carries a GOLD (for Golgi dynamics) domain (23) found

This work was supported in part by grants from Philip Morris, Inc., and Philip Morris International to V.S. and by Grant HL-070583 from the National Institutes of Health to F.A.K.

Manuscript received 8 January 2008 and in revised form 4 February 2008.

Published, JLR Papers in Press, February 11, 2008.

DOI 10.1194/jlr.M800007-JLR200

Copyright © 2008 by the American Society for Biochemistry and Molecular Biology, Inc.

This article is available online at <http://www.jlr.org>

¹ To whom correspondence should be addressed.

e-mail: esoupene@chori.org

§ The online version of this article (available at <http://www.jlr.org>) contains Supplementary data in form of two figures.

in proteins acting as adaptors between membranes and other proteins. ACBD3 interacts with the membrane protein GOLGA3 (or Golgin-160) present on the cytoplasmic face of the Golgi complex (13, 24). As mentioned, in neural stem cells, ACBD3 is released into the cytosol during mitosis, where it interacts with Numb signaling components (12). The last three ACBD members have not been characterized. The C terminus of member 5 is predicted to carry a transmembrane segment and a short coiled-coil motif, whereas two ankyrin-repeat motifs (ANK), which also mediate protein-protein interaction, are predicted for member 6. Similarly, the ACBP members of Arabidopsis differ at the C terminus. ACBP1 and ACBP2 also have ANK repeats and are membrane-associated. ACBP2 was shown to interact with AtEBP via its ANK domain (14). ACBP4 and ACBP5 carry Kelch motifs.

We characterized member 6 of the human family and established that ACBD6 specifically binds long-chain acyl-CoAs with a preference for long and unsaturated acyl chains. Removal of the second half of the protein carrying the ANK motifs does not affect the binding capacity of ACBD6. In *Escherichia coli*, the full-length recombinant protein and the truncated ANK version were soluble and found in the cytosolic fraction. The version truncated of the ACB domain was insoluble. Expression of ACBD6 appears restricted to tissues rich in hematopoietic stem cells (placenta, spleen, and bone marrow) as well as in circulating erythrocyte progenitors (CD34⁺) cells. In placenta, ACBD6 protein was localized in cells surrounding blood vessels representing hemangioblasts, primitive precursors of both blood and vessels. Hematopoietic progenitor cells present in blood in placenta also expressed ACBD6. Although the physiological function of this protein is not known, we propose that human ACBD6 represents a cellular marker for primitive progenitor cells with functions in hematopoiesis and vascular endothelium development.

MATERIALS AND METHODS

DNA and RNA manipulations

A cDNA clone encoding the full-length product of human ACBD6 (gene identifier 84320, GenBank accession number BC006505) was obtained from the American Type Collection Center (ATCC 5299123). The identity of the clone was confirmed by sequencing. A PCR fragment encoding the full-length open reading frame was cloned into the expression vector pET28a (Novagen), with a unique in-frame hexahistidine tag at the C terminus. Amplification was performed with the primer pair Hs.ACBD6-Nco (5'-GGCCATGGCTTCATCATTCTGC-3') and Hs.ACBD6-Xho (5'-AACTCGAGCCTTGCCAGTTGTGTGC-3'), which introduced unique restriction sites for *Nco*I and *Xho*I, respectively (restriction sites are underlined). The ~0.85 kb PCR fragment was cloned with the Zero-Blunt® PCR cloning kit (Invitrogen), according to the manufacturer's instructions, to yield plasmid pFK135. After confirmation by sequencing, the ~0.85 kb *Nco*I-*Xho*I fragment was ligated to pET28a opened by *Nco*I and *Xho*I, to yield plasmid pFK136. Deletions of the acyl-CoA binding domain (residues 1–186) and of the two ANK motifs (residues 188 to the C terminus) were performed by PCR using the primer pair Hs.ACBD6-Xho and Hs.ACBD6-529 (5'-

GGCCATGGCCATCAAATCGAAAAATGTG-3') and the pair Hs.ACBD6-Nco and Hs.ACBD6-534 (5'-AACTCGAGGATGGC-TTTGGTTATATGGTC-3'), respectively. Fragments were cloned into vector pET28a, as described for the full-length construct, to yield plasmids pFK156 and pFK153, respectively.

Total RNA isolation was performed with Totally RNA™ (Ambion, Inc.). RT-PCR amplifications were performed with the SuperScript™ III One-Step RT-PCR System with Platinum® Taq DNA polymerase (Invitrogen). Primer sets used for the full-length cDNA synthesis and amplification of human *ACBD1* (358 bp), *ACBD2* (1,066 bp), *ACBD3* (948 bp), *ACBD4* (886 bp), *ACBD5* (860 bp), and *ACBD6* (856 bp) were as follows: Hs.ACBD1-fwd (5'-CCCTGTCTGACACCGAGCTATGTGG-3') and Hs.ACBD1-rev (5'-GGCACAGTAACCAAATCCAGTCTCT-CATATCCCG-3'), Hs.ACBD2-fwd (5'-CAGCTGCACATGAATA-GAACAGCAATGAGAGCC-3') and Hs.ACBD2-rev (5'-GCATT-TGTGCATTCATCTGATAGCCATCTTCCC-3'), Hs.ACBD3-fwd (5'-TGGAGGAGTTGTACGGCCTGGCACTGC-3') and Hs.ACBD3-rev (5'-CGGCCCACTGTAATCACGGAATCTGC-CATCC-3'), Hs.ACBD4-fwd (5'-ACCGAGAAAGAAAGCCC-AGAGCCCGACTGC-3') and Hs.ACBD4-rev (5'-CGGAAGAGC-CACTGGACGACGAAGGGCCAC-3'), Hs.ACBD5-fwd (5'-CAACACTGGCAGCTGGAGATGGCGG-3') and Hs.ACBD5-rev (5'-GCTGTCTAAAGACTCTTGTGCCAAATTGTTCC-3'), and Hs.ACBD-ATG (5'-ATGGCTTCATCATTCTGCCCCGCGGG-3') and Hs.ACBD-end (5'-CTTTTGATTAAGCCTTGCCAGTTGT-GTGCCGCTGC-3'), respectively. As mentioned in the legend to Fig. 6, some cDNAs of *ACBD6* were reamplified with High-Fidelity Platinum® Taq DNA polymerase (Invitrogen) using primers Hs.ACBD-ATG and Hs.ACBD-rev (5'-GGCTTTGGTTA-TATGGTCAATGTTGTTTCCCTGC-3'), which produced an amplicon of 531 bp. Fragments were cloned with the TA Cloning® kit (Invitrogen) according to the manufacturer's instructions and were sequenced to confirm their identity.

Protein expression and membrane preparation

Full-length ACBD6 and truncated isoforms were expressed in the *E. coli* host BL21 (DE3) cells (Novagen) with 0.2 mM isopropyl β-thiogalactopyranoside for 3 h as described previously (25). Protein sample preparation, cell fractionation, and detection of hexahistidine fusion proteins were performed as described (25).

Purification and gel filtration

The soluble fraction, obtained as described above from 200 ml of culture in 5 ml of Breakage Buffer (0.2 M Tris-HCl, pH 7.4, and 0.1 mM PMSF), was adjusted to 0.3 M NaCl, 10 mM Na-imidazole, pH 7.5, and 2 mM β-mercaptoethanol and mixed with 1.5 ml of nickel-nitrilotriacetic acid agarose slurry (Qjagen). Binding was performed with rotation at 4°C for 16 h. The resin was transferred to an empty column and washed with 30 volumes of the same buffer. Step-wise elutions were performed with 2 volumes of buffer adjusted to increasing concentrations of imidazole (50–500 mM). Full-length ACBD6 and ACBD6-ΔC protein were eluted with 50 and 100 mM imidazole, respectively. The purified proteins were dialyzed for 20 h at 4°C in storage buffer [50 mM Tris-HCl, pH 8.0, 0.2 M NaCl, 2 mM MgCl₂, 1 mM DTT, 5 mM EDTA, and 10% (v/v) glycerol] and stored at –80°C. Another batch of the protein was purified using the His Gravi-Trap kit from Amersham, according to the manufacturer's instructions, and PD-10 columns were used to exchange the buffer of the eluted fraction. As determined by serial dilution on SDS-PAGE gels, both proteins appeared to be ≥90% pure. Gel filtration of purified ACBD6 was performed in the buffer used for the isothermal titration experiments (see below) in 25 mM ammonium acetate, pH 6.0, with 50 mM NaCl, using Bio-Gel

A-1.5m (Bio-Rad) resin, in a 28 × 0.8 cm column. The column was calibrated with gel filtration standard (Bio-Rad), and 3 mg of ACBD6 (60 μl at 50 μg/μl) was applied. Fractions of five drops each were collected, and the absorbance was read at 280 nm. Some fractions were also analyzed by SDS-PAGE to confirm the presence of the protein.

Binding assays

Binding of radiolabeled [¹⁴C]acyl and [¹⁴C]acyl-CoA (C16:0, C18:1, and C20:4) to purified proteins determined by Lipidex-1000 resin (26) was performed as described (27). Briefly, increasing concentrations of ligand (0.2–10 μM) were incubated with 0.1 μM protein at 37°C for 20 min in 200 μl of 10 mM potassium phosphate, pH 7.4 [containing 0.01% Triton X-100 for the assays performed with fatty acids (28, 29)]. Tubes were chilled on ice for 10 min before the addition of 400 μl of ice-cold 50% Lipidex-1000 slurry and were then incubated on ice

for another 20 min. After centrifugation at 12,000 g for 10 min at 4°C, the supernatant ([¹⁴C]acyl-CoA bound to protein) and the resin ([¹⁴C]acyl-CoA bound to Lipidex-1000) were collected, and radioactivity present in the two fractions was determined with a liquid scintillation counter.

Binding of acyl-CoA (C16:0, C18:1, and C20:4) to purified ACBD6 determined by isoelectric focusing gels was performed as described previously (30). Reactions were performed with 100 pmol of ACBD6 in 26 μl of 10 mM potassium phosphate, pH 7.4, in the presence of 300 pmol (3×) or 3,000 pmol (30×) of ligand at 37°C for 10 min. Glycerol was added to a final concentration of 5% (v/v), and samples were loaded directly on pH 3–10 isoelectric focusing gels (Bio-Rad). After isoelectric focusing, according to the manufacturer's instructions, separated complexes were electrotransferred to a polyvinylidene difluoride membrane and blotted with an anti-histidine antibody.

Binding of C18:1-OH and C18:1-CoA was also determined by microcalorimetry titration with a VP-ITC instrument (MicroCal,

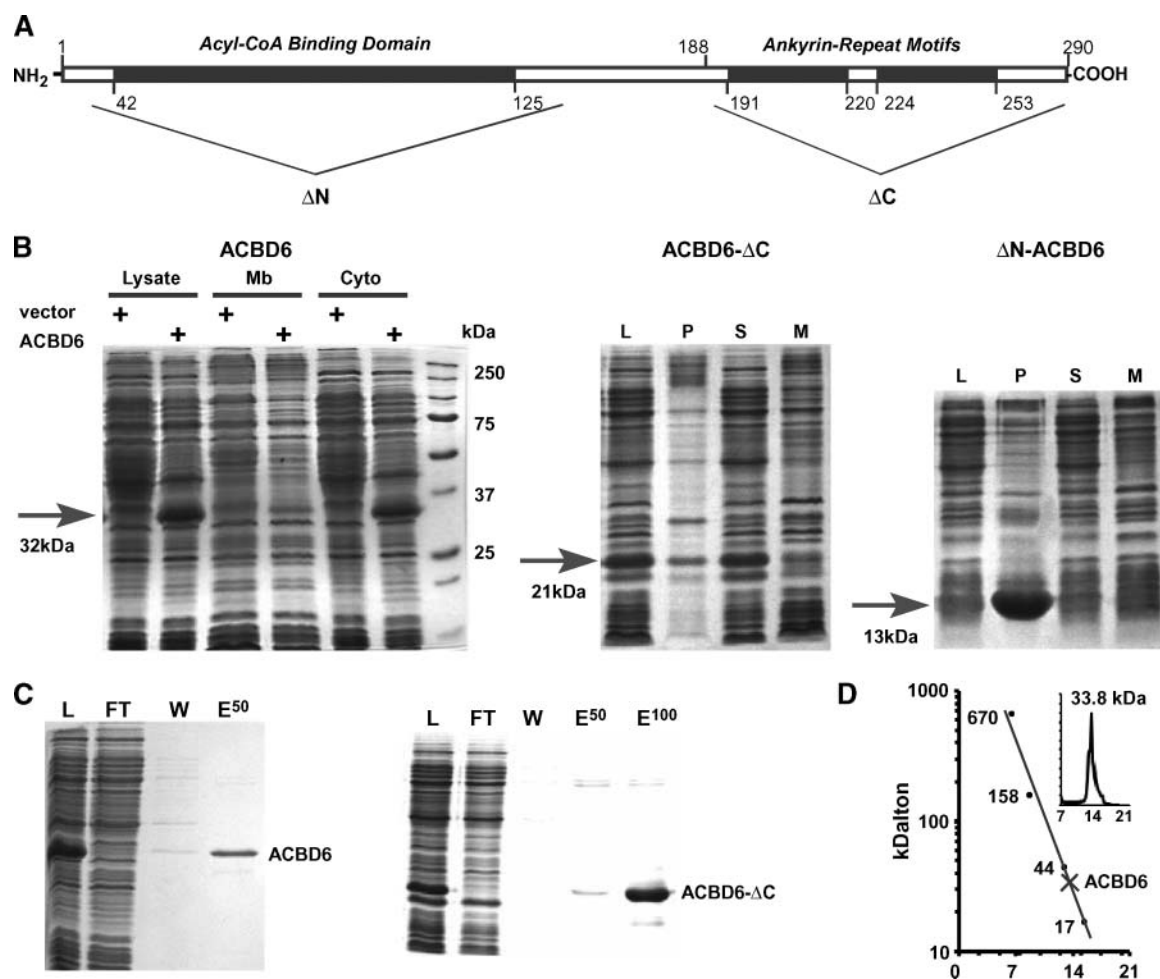


Fig. 1. Expression and purification of human acyl-coenzyme A binding domain-containing member 6 (ACBD6). A: Cartoon representing the full-length protein and the recombinant forms truncated of the acyl-CoA binding domain (Δ N) or of the ankyrin-repeat (ANK) domain (Δ C). The three constructs were expressed with a hexahistidine tag at the C terminus in *E. coli*. B: Detection of ACBD6 proteins expressed in *E. coli*. Proteins were separated on denaturing SDS-PAGE gels and stained with Coomassie blue (see Materials and Methods). Mb, membrane fraction; Cyto, cytosolic fraction; L, lysate; P, insoluble pellet; S, soluble fraction; M, membrane fraction. The positions of the three forms are indicated with arrows, and the calculated molecular mass (kDa) of each is also indicated. In each case, Western blot analysis with an anti-histidine antibody was performed to confirm the identity of the bands. C: Metal-affinity purification of ACBD6 and ACBD6 Δ C proteins. L, extract loaded on a nickel-nitrilotriacetic acid agarose column; FT, flow through; W, wash; E, imidazole elution (50 and 100 mM, as indicated). D: Gel filtration of purified ACBD6 on Bio-Gel resin. The column was calibrated with the indicated molecular mass standards, and the molecular mass of ACBD6 was estimated at 33.8 kDa. The inset shows the elution profile.

LLC). Water, methanol (5%), and RNase-CMP calibration experiments were performed before isothermal titration with ACBD6. All experiments were performed in 25 mM ammonium acetate, pH 6.0, supplemented with 0.1% Triton X-100 when fatty acid was used, at 27°C with 28 injections of 10 μ l every 150 s and constant stirring at 300 rpm. Several sets of experiments were performed with the ligand present in the syringe (300 μ l at 5 mM) or in the cell (1.6 ml at 12.5 μ M) with either purified ACBD6 or fatty acid-free BSA (Sigma) in the cell at 25 μ M or in the syringe at 125 μ M, respectively. Control experiments were run by injecting buffer into the cell containing either the ligand or the protein and by injecting the ligand or protein into the cell containing buffer. Heat generated from control runs was subtracted from the data of the experiment performed under the same conditions.

Immunodetection

A rabbit polyclonal antibody was raised against a peptide of human ACBD6, LDPGWNPQIPEKKGKEC (YenZym Antibodies, LLC, Burlingame, CA), and was affinity-purified. Detection of ACBD6 recombinant proteins expressed in *E. coli* was performed in TBS, 0.1% Tween-20, 1% milk, and anti-ACBD6 at a 1:1,000 dilution for 2 h at room temperature, followed by incubation with a HRP-conjugated goat anti-rabbit IgG under the same conditions. Detection of ACBD6 on a MegaWestern protein array (human adult normal tissues; Biochain Institute, Inc.) was performed as follows: membrane was hydrated for 1 h in TBS with 0.1% Tween-20 for 1 h at room temperature and then blocked for 1 h in 100 ml of TBS with 0.1% Tween-20 and 5% BSA. Primary and second-

ary antibodies were diluted 1:10,000 in 10 ml of TBS with 0.1% Tween-20 and incubated for 2 h. Detection was performed with the Attaglow kit (without enhancement treatment) according to the manufacturer's instructions (Biochain Institute, Inc.).

Immunohistochemistry

After institutional review board approval and informed consent were secured, human term placentas were obtained from healthy females after cesarean section at Alta Bates Medical Center in Berkeley, CA. Only freshly obtained placentas, drained substantially of all cord blood by a conventional collection process, were used. They were infused with an anticoagulant and vasodilator solution (30 U/ml heparin and 1 mg of papaverin hydrochloride) at room temperature. The tissue was then fixed in 2.4% paraformaldehyde for 24 h, washed with PBS, pH 7.4, embedded in paraffin, and sectioned. Before immunostaining, paraffin sections were deparaffinized in xylene (Sigma), rehydrated in alcohol, and washed in PBS. Antigen retrieval was performed with protease K (20 U/ml in 10 mM Tris-HCl pH 7.5, 1 mM EDTA buffer) for 3 min at room temperature. Sections were then incubated with a blocking solution containing 2% goat serum, 3% fetal calf serum, 0.1% Tween-20, and 3% BSA in 4 \times saline-sodium citrate for 60 min at 37°C. They were then incubated with the primary antibody at a 1:100 dilution overnight at 4°C. Sections were washed, incubated with the blocking solution for 20 min, and then incubated with a secondary antibody at a 1:500 dilution for 60 min at 37°C. This antibody was labeled with either FITC or Alexa Fluor 633, as indicated in the figure legends. Finally, sections were washed and mounted

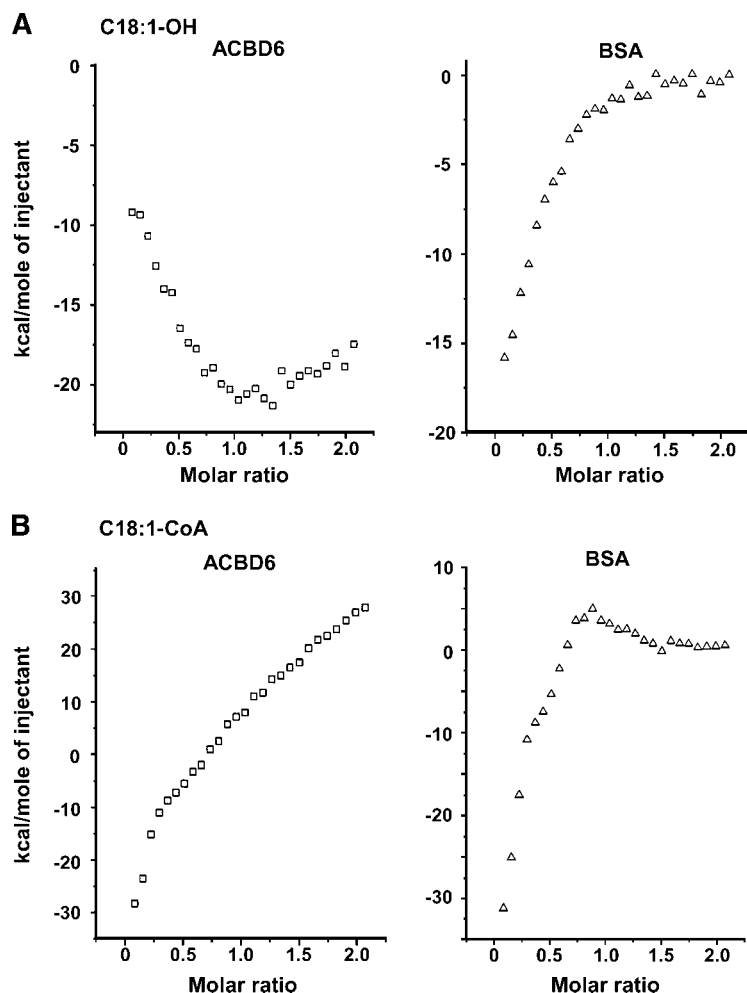


Fig. 2. Isothermal calibration titration of the binding of fatty acid (A) and acyl-CoA (B). Experiments were performed on a VP-ITC instrument with ligands at a concentration of 5 mM injected into the chamber containing 25 μ M ACBD6 (left panels) or BSA (right panels) (see Materials and Methods). Heat generated in the absence of each of the two components was determined and subtracted from the raw data, which are presented in supplementary Fig. I.

on slides with Gold Antifade reagent (Molecular Probes, Invitrogen, Carlsbad, CA). The following antibodies were used: mouse anti-human CD34 (No. 555820; BD Pharmingen, San Jose, CA), mouse anti-human CD31 (No. BM4047; Acris Antibodies GmbH), rabbit anti-human CD133 (No. ab16518; Abcam, Cambridge, MA), rat anti-human SSEA-3 (No. ab16286; Abcam), rabbit anti-human Oct-4 (No. ab19857; Abcam), and rabbit anti-human Nanog (No. ab21603; Abcam). Isotype anti-mouse and anti-rabbit antibodies were from Zymed (South San Francisco, CA). Secondary anti-mouse and anti-rabbit FITC- or Alexa Fluor 633-labeled antibodies were from Molecular Probes, Invitrogen.

Primary cultures of placental stromal plastic-adherent cells

A part of the placenta was isolated with clamps, and the arterial vessels were washed with 50 ml of PBS and infused with 50 ml of PBS containing a penicillin-streptomycin-fungisone (PSF) cocktail (100 U/ml penicillin, 100 µg/ml streptomycin, and 0.25 µg/ml fungisone; Invitrogen), 2.5 U/ml Dispase, 0.5 mg/ml trypsin, and 2 g/l EDTA for 20 min at 37°C. The tissue was dissected to samples of 1–5 g, which were thoroughly washed three times with 100 ml of sterile PBS with PSF cocktail and heparin at 30 U/ml. Small pieces (1 × 3 × 3 mm) were cut, placed in 1 ml (~10 times the volume of the pieces) of PBS containing 0.1% Collagenase I (Sigma) and 2.5 U/ml Dispase, and digested for 30 min at 37°C. They were then vortexed for 5 min and centrifuged at 400 g for 15 min. The supernatant was discarded. The cell pellet was suspended in α-MEM with PSF, 15% fetal calf serum, and 2 mM L-glutamine and transferred in Petri dishes to a growth incubator. After 24 h, the cells were washed twice with PBS, and fresh growth medium was added. Plastic-adherent cells were grown for 2–3 weeks in α-MEM with PSF, 15% fetal calf serum, and 2 mM L-glutamine. Immunostaining of cell cultures was performed as described above. In addition to staining for CD133, immunofluorescent staining was performed for markers of human embryonic stem cells Oct-4, Nanog, and SSEA-3. Cell differentiation was performed as described (31, 32).

RESULTS AND DISCUSSION

Expression and purification of ACBD6

ACBD6 is a 32 kDa protein that is predicted by sequence analysis to carry an ACB domain between residues 42 and 125 and two ANK motifs at its C terminus (Fig. 1A). The presence of ANK motifs is unique to this member of the family. The full-length ACBD6 protein was expressed successfully in *E. coli* and was detected only in the soluble fraction (Fig. 1B). The form truncated of the C terminus, ACBD6-ΔC, was also soluble, whereas removal of the N terminus, ΔN-ACBD6, resulted in an insoluble protein (Fig. 1B). The two soluble forms, full-length ACBD6 and ACBD6-ΔC, were purified by affinity chromatography (Fig. 1C). The molecular mass of the purified full-length protein was determined under native conditions by gel filtration. Recombinant ACBD6 eluted as a single peak with an estimated mass of 33.8 kDa, for a calculated molecular mass of 32.2 kDa (Fig. 1D). Thus, the purified protein was in a monomeric state.

Isothermal calorimetric titration assays

We used the isothermal calorimetric titration technique to test the binding of free fatty acids and acyl-CoAs to the

purified ACBD6 protein. Control assays performed either in the absence of the ligand or in the absence of the protein resulted in significant heat generation and in complex titration patterns (see supplementary Fig. I). In contrast to the well-defined saturation profile obtained for BSA and long-chain fatty acid, C18:1-OH, no binding for fatty acid could be established for ACBD6 (Fig. 2A). However, binding to C18:1-CoA was detected both when the ligand was in the injection syringe (Fig. 2B) and when it was present in the chamber (Fig. 3). This technique has been used previously to study the binding of acyl-CoA to the ACBP protein (ACBD1), but the transition from the unbound to the saturated-bound state was observed in a single injection of the ligand (27). For ACBD6, the titration curves were also difficult to interpret, and they could not be fitted to a single binding constant model. When the protein was titrated into the chamber containing the ligand (Fig. 3), the isothermal titration profile resolved in a characteristic system of sites with two different binding constants (I and II), in which binding to the site(s) of low affinity (II) occurs only after saturation of the site(s) with higher affinity (I).

Acyl-CoA binding characteristics

The binding activity of ACBD6 and of the ΔC-truncated form that only contains the ACB domain was determined by the Lipidex-1000 technique for acyl-CoAs of different chain lengths and degrees of unsaturation (26, 28, 33–35).

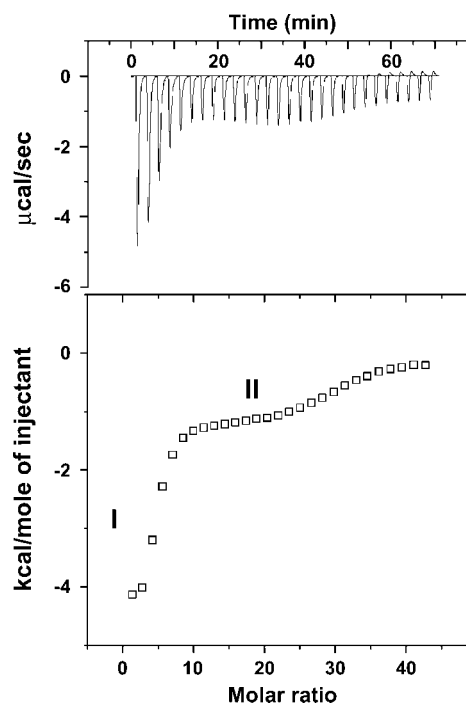


Fig. 3. Binding mode of oleoyl-CoA to ACBD6. Isothermal calibration titration of ACBD6 (125 µM) injected into the chamber containing C18:1-CoA at 12.5 µM. Data were normalized as described for Fig. 2. Raw data are shown in supplementary Fig. I. The putative sites with two different binding affinities are indicated (I and II) in the lower panel.

As shown in Fig. 4, recombinant ACBD6 binds all three acyl-CoA species tested. Binding was stronger for C18:1-CoA than for C20:4-CoA and was very weak for the shorter and saturated C16:0-CoA. This apparent substrate preference was independently confirmed by the detection of the acyl-CoA:ACBD6 complexes on isoelectric focusing gels (30). At a 30:1 molar ratio (ligand-protein), all three acyl-CoAs bound and saturated the protein (see supplementary Fig. II). At a lower concentration, a 3:1 molar ratio, ACBD6 was still bound to C18:1-CoA and C20:4-CoA but no binding was detected for C16:0-CoA. Thus, ACBD6 appeared to have a lower affinity for palmitoyl-CoA compared with the

longer and unsaturated oleoyl- and arachidonoyl-CoAs. No binding for fatty acids was detected.

Removal of the two ANK motifs, ACBD6- Δ C, had no effect on the binding activity or on the substrate preference (Fig. 4). Thus, the ACB domain present at the N terminus is sufficient for binding to the substrate. From the data obtained from these assays, the binding constant for C18:1-CoA was calculated at 3.5 μ M (Fig. 4), with an unexpected Bmax (for number of sites) of 4 (mol ligand/mol protein).

The stoichiometry of acyl-CoA binding proteins was often proposed to be 1 mol of ligand for 1 mol of protein, but the recently described structure of the human liver ACBP (ACBD1) protein bound to myristoyl-CoA revealed a more complex binding characteristic. One acyl-CoA molecule was bound to one of the two ACBP units of the dimeric complex via its acyl chain, but it was also bound to the second ACBP unit by its 3'-phosphate-ribose moiety (19). In addition, part of other acyl-CoA molecules present in the crystal filled the unoccupied space of the binding pocket of each of the two units. The stoichiometry of fatty acid binding protein (FABP) is also diverse. Liver FABP was determined at a 2:1 ratio (ligand-protein), whereas intestinal FABP was determined at a 1:1 ratio. ACBD6 appeared to be a monomer, to contain two classes of sites, and to bind four molecules of ligand. As shown for ACBD1 and BSA, the binding of long-chain acyl-CoAs to ACBD6 is complex.

ACBD6 is expressed in hematopoietic tissues

An affinity-purified antibody was produced against human ACBD6 and used to determine the presence of the protein in 30 different human tissues by Western blot analysis (see Materials and Methods). The ACBD6 protein was detected only in placenta and in spleen (note that cord blood and bone marrow were not represented in this protein array; see legend to Fig. 5). Although ACBP proteins are abundant in brain and liver and can represent up to 8% of total soluble proteins in some cells (1), ACBD6 was not detected in those tissues (Fig. 5, lanes 6, 19).

The presence of ACBD6 mRNA in placenta and other hematopoietic tissues and cells was confirmed by RT-PCR. ACBD6 mRNA was detected in total RNA isolated from CD34⁺ erythrocyte progenitors, cord blood, placenta, and bone marrow (Fig. 6A). It was also detected in cultured undifferentiated placenta-derived stromal embryo-like cells and in the erythropoietic cell line K562 (Fig. 6B, C). Mining of the HemBase database (36, 37) (library identifier 11923) confirmed the presence of ACBD6 in erythrocyte precursor cells. No other member of the ACBD family was identified. Thus, ACBD6 expression appeared to be restricted to tissues rich in hematopoietic stem cells.

Placenta-derived stromal embryonic-like stem cells express ACBD6

We established several lines of plastic-adherent cells from human placentas. These cells were negative for CD45, CD34, and CD38 and propagated up to 100 dou-

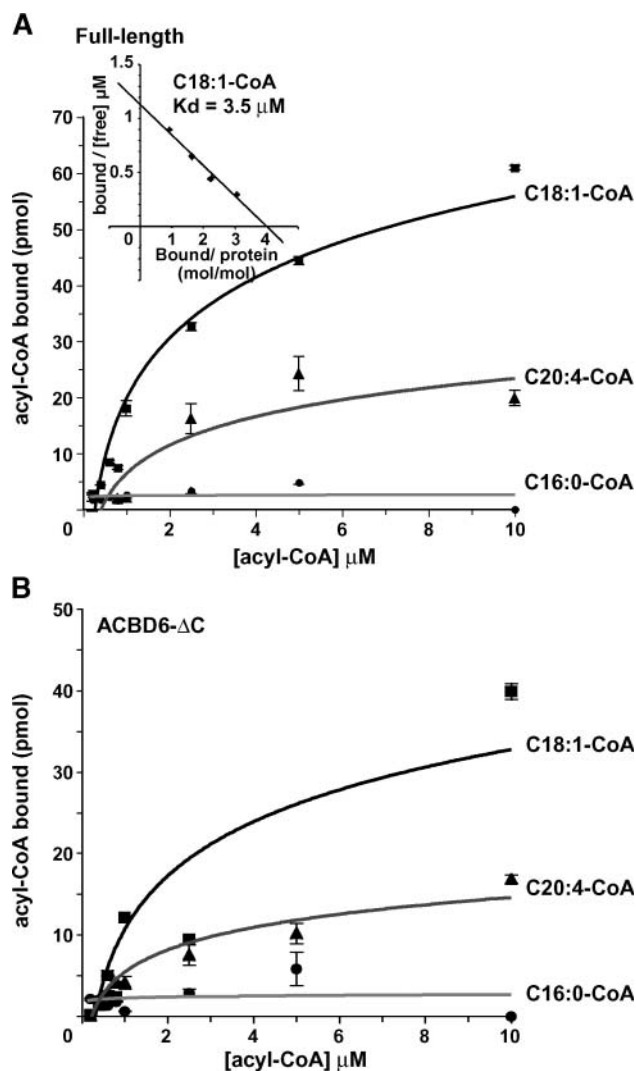


Fig. 4. Acyl-CoA binding determinant and preference. Binding assays were performed with the purified full-length ACBD6 (A) and the form truncated of the ANK motifs (ACBD6- Δ C; B). Assays were performed with 0.1 μ M protein and the indicated ¹⁴C-labeled acyl-CoA species at increasing concentrations from 0.2 to 10 μ M. Unbound ligand was removed with Lipidex-1000 resin as described in Materials and Methods. Error bars represent the SD of three different experiments. The inset shows a Scatchard plot representing ligand bound to free ligand concentration as a function of ligand bound to protein amount. Binding affinity (Kd) and number of sites (Bmax) were calculated by nonlinear regression using Prism4 software (GraphPad Software, Inc.).

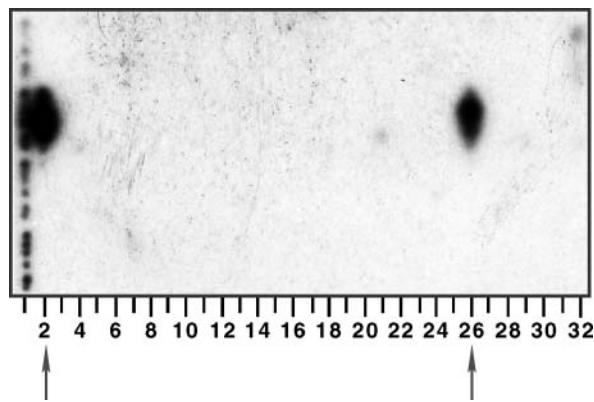


Fig. 5. Detection of ACBD6 protein in human tissues. Western blot analysis was performed with an affinity-purified ACBD6 antibody on a MegaWestern protein array (Biochain Institute, Inc.) representing 30 different human adult normal tissues (see Materials and Methods). Protein was detected within 1 min of exposure, and results after 5 min are shown. Note that signal was detected only in lanes 2 and 26 (arrows), corresponding to placenta and spleen tissues, respectively. A control sample used for the orientation of the array is in lane 1, and a negative control (no protein loaded) is in lane 3. The tissues represented were as follows: lane 2, placenta; lane 4, adipose; lane 5, bladder; lane 6, brain; lane 7, breast; lane 8, cerebellum; lane 9, cervix; lane 10, colon; lane 11, diaphragm; lane 12, duodenum; lane 13, esophagus; lane 14, gallbladder; lane 15, heart; lane 16, ileum; lane 17, jejunum; lane 18, kidney; lane 19, liver; lane 20, lung; lane 21, ovary; lane 22, pancreas; lane 23, rectum; lane 24, skeletal muscle; lane 25, skin; lane 26, spleen; lane 27, stomach; lane 28, testis; lane 29, thymus; lane 30, thyroid; lane 31, tonsil; and lane 32, uterus.

blings in cell culture. They can differentiate into adipocytes, osteoblasts, and neurons in adipogenic, osteogenic, and neurogenic media, respectively (V. Serikov and F. A. Kuypers, unpublished data). They were highly positive for Oct-4, Nanog, and SSEA-3, classical markers of human embryonic stem cells (Fig. 7 and data not shown). The full-length ACBD6 mRNA was detected in these cell lines (Fig. 6B). The presence of the protein was confirmed by histolocalization on fixed cells (Fig. 7). The other five ACBD members were also detected by RT-PCR, indicating that these cultured embryonic stem cells expressed all six members of the family (data not shown).

Expression of ACBD6 in placenta is restricted to primitive stem cells

Immunolocalization of ACBD6 on cryosections of human placenta confirmed the presence of ACBD6 in this tissue (data not shown). Immunocytochemistry detection performed on paraffin-embedded placenta sections established that ACBD6 was present in hematopoietic progenitor CD34⁺ cells (Fig. 8A). Thus, expression of ACBD6 in CD34⁺ cells was established at both the mRNA and protein levels. In addition, the protein was detected in some endothelial cells (CD31⁺) surrounding the blood vessels (Fig. 8B). Those cells were also positive for the marker of primitive hematopoietic stem cells, CD133⁺ (Fig. 8C). These CD31⁺/CD133⁺ cells represent hemangioblasts, which are the primitive precursors of both blood and vessels.

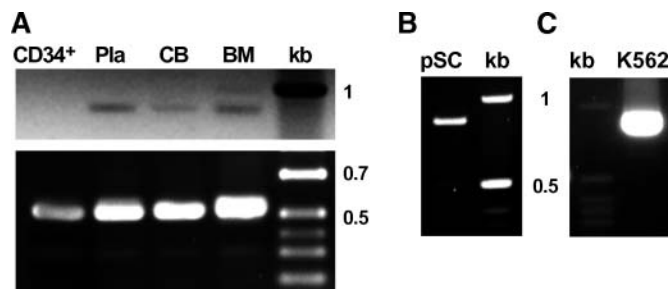


Fig. 6. ACBD6 mRNA detection in tissues and cells. Reverse transcriptions of full-length ACBD6 of total RNA isolated from CD34⁺ positive cells (CD34⁺), placenta (Pla), cord blood (CB), and bone marrow (BM) tissues (A), from placenta-derived stem cells (pSC) (B), and from K562 cells (C). Full-length amplification is shown in the upper panel in A. Nested reamplification of these full-length cDNA products is shown in the lower panel, and they represent partial cDNA sequences. Note that very low amounts of total RNA were used (<ng; see Materials and Methods), and no signal could be seen without reamplification of the CD34⁺ cDNA. The identity of all cDNA products was verified by sequencing.

Vascular development in placenta, vasculogenesis, which is the formation of the first blood vessels, and angiogenesis, the further development of new vessels, is the result of the differentiation of pluripotent mesenchymal cells into hemangiogenic stem cells (38, 39). Apoptosis of vascular endothelial cells affects the growth of blood vessels and provides the means for vascular branching and remodeling during angiogenesis (40–44). ACBD6 is present in endothelial cells surrounding the blood vessels positive for markers of hemangiogenic stem cells. As established, ACBD6 binds unsaturated acyl-CoA, with a strong preference for oleoyl-CoA, but has a very low binding capacity for the saturated palmitate derivative, palmitoyl-CoA. Fatty acids, in particular long-chain fatty acids, can act as signaling molecules and regulate gene expression (45). They can also affect the processes of apoptosis and the activation of vascular endothelial cells (46–49). Intriguingly, saturated (palmitic acid) and unsaturated (oleic acid) fatty acids have distinct and sometimes opposite effects on such processes (46, 48). Although fatty acids can bind directly to various regulators, such as nuclear receptors, their CoA ester derivatives produced intracellularly by the action of long-chain acyl-CoA synthetases have been proposed to represent the active species in some instances (45, 46, 48). Altogether, the activity and restricted expression profile of ACBD6 in placenta could indicate that ACBD6 functions in vascular endothelium development in placenta. It potentially could be involved in controlling the effect of long-chain fatty acids through binding to their CoA ester derivatives. As mentioned in the introduction, members of the acyl-CoA binding family have been found to interact with other proteins, in particular receptors and regulatory proteins. ACBD6 carries two ANK motifs that are often involved in protein-protein interaction. ACBP2 of plants, which also carries such a motif, was shown to interact with the ethylene-responsive element. Thus, the extended C terminus of ACBD6, which is dispensable for binding to

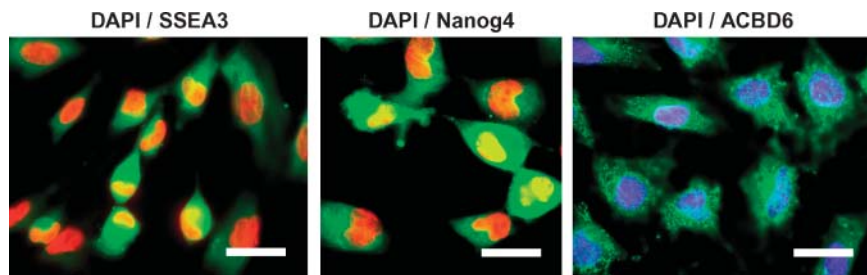


Fig. 7. Detection of ACBD6 protein in cultured placenta-derived stem cells. Embryonic-like stem cells were isolated from human placenta and grown as described in Materials and Methods. Immunostaining for the stem cell markers SSEA3 and Nanog is shown in green merged with 4',6-diamidino-2-phenylindole (DAPI) staining in red (pseudocolor), and staining for ACBD6 is shown in green merged with DAPI staining in blue (true color). Bars = 5 μ m. Expression of all three proteins indicates that ACBD6 is a marker of primitive stem cells.

the ligand, might represent a domain interacting with other protein(s).

In conclusion, ACBD6 is an acyl-CoA binding protein that is expressed in hematopoietic tissues and appears to

be restricted to primitive stem cells present in those tissues. In neural stem cells, ACBD3 has been shown to mediate cell fate specification, self renewal versus neuronal differentiation, through binding to components of

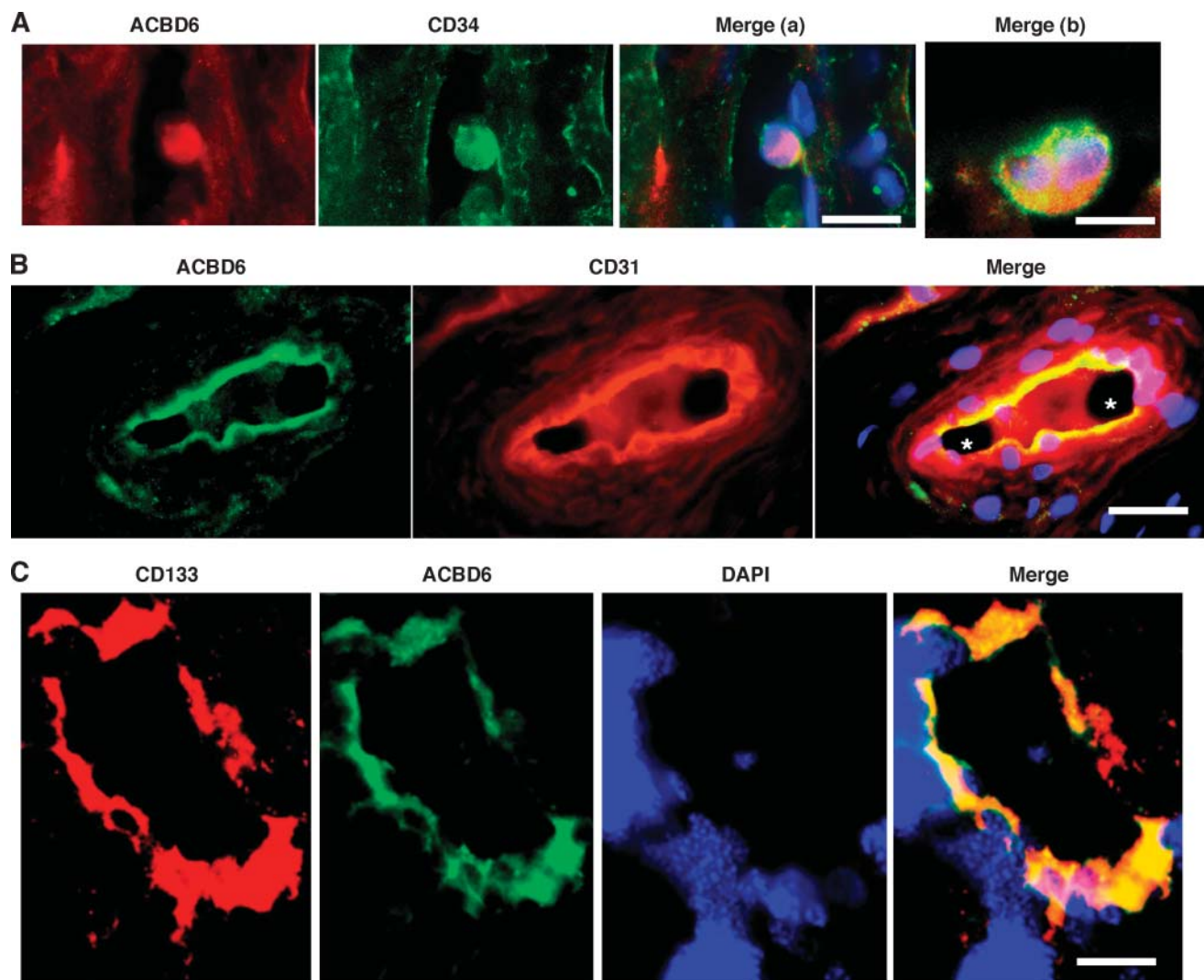



Fig. 8. Colocalization of ACBD6 protein with CD31⁺, CD34⁺, and CD133⁺ cells in placenta. Paraffin-embedded sections of human placenta were stained for ACBD6 (red) and CD34 (green) in A, for ACBD6 (green) and CD31 (red) in B, and for ACBD6 (green) and CD133 (red) in C. In each case, the merged image also shows DAPI staining in blue. Merged images of two different ACBD6⁺/CD34⁺ cells are shown in A (a, b). Two blood vessels are indicated with asterisks in the merged image of B. Bars = 10 μ m (Aa, C) 5 μ m (Ab), and 15 μ m (B).

Numb signaling (12). ACBD6 is produced in cultured embryonic-like stem cells derived from placenta. Those stem cells can undergo differentiation into three cell types in the presence of the appropriate stimuli and represent a cell line system in which to study the function of ACBD6 in stem cells. However, these studies might be complicated by the finding that small interfering RNA downregulation of ACBD1 in HeLa cells was lethal as a result of defects in thymidine and acetate metabolism (50). 

REFERENCES

- Burton, M., T. M. Rose, N. J. Faergeman, and J. Knudsen. 2005. Evolution of the acyl-CoA binding protein (ACBP). *Biochem. J.* **392**: 299–307.
- Gossett, R. E., A. A. Frolov, J. B. Roths, W. D. Behnke, A. B. Kier, and F. Schroeder. 1996. Acyl-CoA binding proteins: multiplicity and function. *Lipids.* **31**: 895–918.
- Knudsen, J., S. Mandrup, J. T. Rasmussen, P. H. Andreasen, F. Poulsen, and K. Kristiansen. 1993. The function of acyl-CoA-binding protein (ACBP)/diazepam binding inhibitor (DBI). *Mol. Cell. Biochem.* **123**: 129–138.
- Kragelund, B. B., J. Knudsen, and F. M. Poulsen. 1999. Acyl-coenzyme A binding protein (ACBP). *Biochim. Biophys. Acta.* **1441**: 150–161.
- Rasmussen, J. T., J. Rosendal, and J. Knudsen. 1993. Interaction of acyl-CoA binding protein (ACBP) on processes for which acyl-CoA is a substrate, product or inhibitor. *Biochem. J.* **292**: 907–913.
- Chao, H., M. Zhou, A. McIntosh, F. Schroeder, and A. B. Kier. 2003. ACBP and cholesterol differentially alter fatty acyl CoA utilization by microsomal ACAT. *J. Lipid Res.* **44**: 72–83.
- Abo-Hashema, K. A., M. H. Cake, M. A. Lukas, and J. Knudsen. 2001. The interaction of acyl-CoA with acyl-CoA binding protein and carnitine palmitoyltransferase I. *Int. J. Biochem. Cell Biol.* **33**: 807–815.
- Faergeman, N. J., and J. Knudsen. 1997. Role of long-chain fatty acyl-CoA esters in the regulation of metabolism and in cell signalling. *Biochem. J.* **323**: 1–12.
- Costa, E., and A. Guidotti. 1991. Diazepam binding inhibitor (DBI): a peptide with multiple biological actions. *Life Sci.* **49**: 325–344.
- Guidotti, A. 1991. Role of DBI in brain and its posttranslational processing products in normal and abnormal behavior. *Neuropharmacology.* **30**: 1425–1433.
- Guidotti, A., C. M. Forchetti, M. G. Corda, D. Konkel, C. D. Bennett, and E. Costa. 1983. Isolation, characterization, and purification to homogeneity of an endogenous polypeptide with agonistic action on benzodiazepine receptors. *Proc. Natl. Acad. Sci. USA.* **80**: 3531–3535.
- Zhou, Y., J. B. Atkins, S. B. Rompani, D. L. Bancescu, P. H. Petersen, H. Tang, K. Zou, S. B. Stewart, and W. Zhong. 2007. The mammalian Golgi regulates numb signaling in asymmetric cell division by releasing ACBD3 during mitosis. *Cell.* **129**: 163–178.
- Sohda, M., Y. Misumi, A. Yamamoto, A. Yano, N. Nakamura, and Y. Ikehara. 2001. Identification and characterization of a novel Golgi protein, GCP60, that interacts with the integral membrane protein giantin. *J. Biol. Chem.* **276**: 45298–45306.
- Li, H. Y., and M. L. Chye. 2004. Arabidopsis acyl-CoA-binding protein ACBP2 interacts with an ethylene-responsive element-binding protein, AtEBP, via its ankyrin repeats. *Plant Mol. Biol.* **54**: 233–243.
- Leung, K. C., H. Y. Li, G. Mishra, and M. L. Chye. 2004. ACBP4 and ACBP5, novel Arabidopsis acyl-CoA-binding proteins with Kelch motifs that bind oleoyl-CoA. *Plant Mol. Biol.* **55**: 297–309.
- Chye, M. L., B. Q. Huang, and S. Y. Zee. 1999. Isolation of a gene encoding Arabidopsis membrane-associated acyl-CoA binding protein and immunolocalization of its gene product. *Plant J.* **18**: 205–214.
- Li, H. Y., and M. L. Chye. 2003. Membrane localization of Arabidopsis acyl-CoA binding protein ACBP2. *Plant Mol. Biol.* **51**: 483–492.
- Leung, K. C., H. Y. Li, S. Xiao, M. H. Tse, and M. L. Chye. 2006. Arabidopsis ACBP3 is an extracellularly targeted acyl-CoA-binding protein. *Planta.* **223**: 871–881.
- Taskinen, J. P., D. M. van Aalten, J. Knudsen, and R. K. Wierenga. 2007. High resolution crystal structures of unliganded and liganded human liver ACBP reveal a new mode of binding for the acyl-CoA ligand. *Proteins.* **66**: 229–238.
- Janssen, U., and W. Stoffel. 2002. Disruption of mitochondrial β -oxidation of unsaturated fatty acids in the 3,2-trans-enoyl-CoA isomerase-deficient mouse. *J. Biol. Chem.* **277**: 19579–19584.
- Kilponen, J. M., P. M. Palosaari, and J. K. Hiltunen. 1990. Occurrence of a long-chain Δ^3, Δ^2 -enoyl-CoA isomerase in rat liver. *Biochem. J.* **269**: 223–226.
- Zhang, D., W. Yu, B. V. Geisbrecht, S. J. Gould, H. Sprecher, and H. Schulz. 2002. Functional characterization of Δ^3, Δ^2 -enoyl-CoA isomerases from rat liver. *J. Biol. Chem.* **277**: 9127–9132.
- Anantharaman, V., and L. Aravind. 2002. The GOLD domain, a novel protein module involved in Golgi function and secretion. *Genome Biol.* **3**: RESEARCH0023.
- Sbdio, J. I., S. W. Hicks, D. Simon, and C. E. Machamer. 2006. GCP60 preferentially interacts with a caspase-generated golgin-160 fragment. *J. Biol. Chem.* **281**: 27924–27931.
- Soupe, E., and F. A. Kuypers. 2006. Multiple erythroid isoforms of human long-chain acyl-CoA synthetases are produced by switch of the fatty acid gate domains. *BMC Mol. Biol.* **7**: 1–12.
- Ellingboe, J., E. Nystrom, and J. Sjovall. 1970. Liquid-gel chromatography on lipophilic-hydrophobic Sephadex derivatives. *J. Lipid Res.* **11**: 266–273.
- Faergeman, N. J., B. W. Sigurskjold, B. B. Kragelund, K. V. Andersen, and J. Knudsen. 1996. Thermodynamics of ligand binding to acyl-coenzyme A binding protein studied by titration calorimetry. *Biochemistry.* **35**: 14118–14126.
- Kerckhoff, C., M. Klempt, V. Kaever, and C. Sorg. 1999. The two calcium-binding proteins, S100A8 and S100A9, are involved in the metabolism of arachidonic acid in human neutrophils. *J. Biol. Chem.* **274**: 32672–32679.
- Vork, M. M., J. F. Glatz, D. A. Surtel, and G. J. van der Vusse. 1990. Assay of the binding of fatty acids by proteins: evaluation of the Lipidex 1000 procedure. *Mol. Cell. Biochem.* **98**: 111–117.
- Knudsen, J., N. J. Faergeman, H. Skott, R. Hummel, C. Borsting, T. M. Rose, J. S. Andersen, P. Hojrup, P. Roepstorff, and K. Kristiansen. 1994. Yeast acyl-CoA-binding protein: acyl-CoA-binding affinity and effect on intracellular acyl-CoA pool size. *Biochem. J.* **302**: 479–485.
- Gupta, N., X. Su, B. Popov, J. W. Lee, V. Serikov, and M. A. Matthay. 2007. Intrapulmonary delivery of bone marrow-derived mesenchymal stem cells improves survival and attenuates endotoxin-induced acute lung injury in mice. *J. Immunol.* **179**: 1855–1863.
- Popov, B. V., V. B. Serikov, N. S. Petrov, T. V. Izusova, N. Gupta, and M. A. Matthay. 2007. Lung epithelial cells induce endodermal differentiation in mouse mesenchymal bone marrow stem cells by paracrine mechanism. *Tissue Eng.* **13**: 2441–2450.
- Mandrup, S., P. Hojrup, K. Kristiansen, and J. Knudsen. 1991. Gene synthesis, expression in *Escherichia coli*, purification and characterization of the recombinant bovine acyl-CoA-binding protein. *Biochem. J.* **276**: 817–823.
- Rasmussen, J. T., T. Borchers, and J. Knudsen. 1990. Comparison of the binding affinities of acyl-CoA-binding protein and fatty-acid-binding protein for long-chain acyl-CoA esters. *Biochem. J.* **265**: 849–855.
- Rosendal, J., P. Ertbjerg, and J. Knudsen. 1993. Characterization of ligand binding to acyl-CoA-binding protein. *Biochem. J.* **290**: 321–326.
- Goh, S. H., Y. T. Lee, G. G. Bouffard, and J. L. Miller. 2004. HemBase: browser and genome portal for hematology and erythroid biology. *Nucleic Acids Res.* **32**: D572–D574.
- Gubin, A. N., J. M. Njoroge, G. G. Bouffard, and J. L. Miller. 1999. Gene expression in proliferating human erythroid cells. *Genomics.* **59**: 168–177.
- Demir, R., U. A. Kayisli, S. Cayli, and B. Huppertz. 2006. Sequential steps during vasculogenesis and angiogenesis in the very early human placenta. *Placenta.* **27**: 535–539.
- Demir, R., Y. Seval, and B. Huppertz. 2007. Vasculogenesis and angiogenesis in the early human placenta. *Acta Histochem.* **109**: 257–265.
- Chavakis, E., and S. Dimmeler. 2002. Regulation of endothelial cell survival and apoptosis during angiogenesis. *Arterioscler. Thromb. Vasc. Biol.* **22**: 887–893.
- Dimmeler, S., and A. M. Zeiher. 2000. Endothelial cell apoptosis in angiogenesis and vessel regression. *Circ. Res.* **87**: 434–439.

42. Hughes, S., and T. Chang-Ling. 2000. Roles of endothelial cell migration and apoptosis in vascular remodeling during development of the central nervous system. *Microcirculation*. **7**: 317–333.
43. Sakamaki, K. 2004. Regulation of endothelial cell death and its role in angiogenesis and vascular regression. *Curr. Neurovasc. Res.* **1**: 305–315.
44. Tertemiz, F., U. A. Kayisli, A. Arici, and R. Demir. 2005. Apoptosis contributes to vascular lumen formation and vascular branching in human placental vasculogenesis. *Biol. Reprod.* **72**: 727–735.
45. Pegorier, J. P., C. Le May, and J. Girard. 2004. Control of gene expression by fatty acids. *J. Nutr.* **134 (Suppl.)**: 2444–2449.
46. Carluccio, M. A., M. Massaro, C. Bonfrate, L. Siculella, M. Maffia, G. Nicolardi, A. Distanto, C. Storelli, and R. De Caterina. 1999. Oleic acid inhibits endothelial activation: a direct vascular anti-atherogenic mechanism of a nutritional component in the Mediterranean diet. *Arterioscler. Thromb. Vasc. Biol.* **19**: 220–228.
47. Ciapaite, J., J. van Bezu, G. van Eikenhorst, S. J. Bakker, T. Teerlink, M. Diamant, R. J. Heine, K. Krab, H. V. Westerhoff, and C. G. Schalkwijk. 2007. Palmitate and oleate have distinct effects on the inflammatory phenotype of human endothelial cells. *Biochim. Biophys. Acta.* **1771**: 147–154.
48. Staiger, K., H. Staiger, C. Weigert, C. Haas, H. U. Haring, and M. Kellerer. 2006. Saturated, but not unsaturated, fatty acids induce apoptosis of human coronary artery endothelial cells via nuclear factor-kappaB activation. *Diabetes.* **55**: 3121–3126.
49. Toborek, M., Y. W. Lee, R. Garrido, S. Kaiser, and B. Hennig. 2002. Unsaturated fatty acids selectively induce an inflammatory environment in human endothelial cells. *Am. J. Clin. Nutr.* **75**: 119–125.
50. Faergeman, N. J., and J. Knudsen. 2002. Acyl-CoA binding protein is an essential protein in mammalian cell lines. *Biochem. J.* **368**: 679–682.